SCIENCE & GLOBAL SECURITY
2023, VOL. 31, NOS. 1–2, 3–15
https://doi.org/10.1080/08929882.2023.2215590

Routledge
Taylor & Francis Group

Radioactive Fallout and Potential Fatalities from Nuclear Attacks on China's New Missile Silo Fields

Sébastien Philippe [a] and Ivan Stepanov[b]

[a]Program on Science and Global Security, Princeton University, Princeton, NJ, USA; [b]Nuclear War Simulator, Published by Slitherine Software, ltd, Stuttgart, Germany

ABSTRACT

China is constructing three new nuclear ballistic missile silo fields near the cities of Yumen, Hami, and Ordos as part of a significant buildup of its nuclear weapon arsenal. Once operational, these missile silos will likely be included as targets in U.S. strategic counterforce war plans. Such plans call for using one or two nuclear warheads to strike each silo. Such attacks can generate large amounts of radioactive debris that are then transported by local winds and can deliver lethal doses of radiation to population hundreds of kilometers away. Here, we compute radioactive fallout from counterforce attacks on the three new alleged missile silo fields using the combination of a nuclear war simulator and modern atmospheric particle transport software and recent archived weather data. We find that the construction of these new silos will put tens of millions of Chinese civilians at risk of lethal fallout including in East China. In particular, the relatively short distance between the Ordos missile field and Beijing and the local winds patterns for the region, suggest that about half of the 21 million inhabitants of the Chinese capital could die following a counterforce strike, even if given advanced warning to shelter in place.

ARTICLE HISTORY
Received 20 October 2022
Accepted 28 April 2023

Introduction

Recent commercial satellite observations show that China has begun the construction of three new intercontinental ballistic missile silo fields near the cities of Yumen, Hami, and Ordos.[1] In total, more than 270 possible silos have been spotted and are under various stages of construction.[2] Once loaded with nuclear-capable ballistic missiles, these three sites are likely to be included as targets in existing U.S. nuclear war plans.[3] Such plans include counterforce options that are aimed at destroying an adversary's deployed nuclear weapons and capacity to retaliate.

Attacking a missile silo requires detonating one or two nuclear warheads at or close to the target that is buried underground. The resulting nuclear

CONTACT Sébastien Philippe sebastien@princeton.edu Program on Science and Global Security, Princeton University, Princeton, NJ, USA.

explosions can generate large radioactive debris clouds that then deposit solid particles carrying the radioactive fission products on downwind areas. While silos are typically located in areas with low population density, previous studies have shown that the fallout resulting from a nuclear attack on these sites can travel hundreds of kilometers putting nearby population centers at risk of receiving lethal doses of radiation.[4]

Here we calculate the nuclear fallout and estimate potential fatalities from counterforce nuclear attacks on the three new Chinese nuclear ballistic missile silo fields for each day of the 2021 calendar year. Building on the existing literature,[5] we combine a modern atmospheric particle transport code[6] with a nuclear war simulation software[7] to compute cumulative dose to the public using archived weather data and identify populations at risk using population density databases.

We find that counterforce attacks on the Yumen, Hami, and Ordos silo fields will put millions of Chinese at risk of lethal doses of radiation. Our results show that an attack on the Ordos missile silo field located ~700 km west of Beijing could deliver a lethal dose of radiation to the inhabitants of the Chinese capital should high altitude winds blow toward the east as they typically do in wintertime. In addition, fallout would also affect neighboring countries leading to additional fatalities in North Korea, South Korea, Mongolia, and Japan among others. Beyond this case-study, the method and software stack developed for this project could be used to simulate nuclear fallout and associated civilian fatalities for other relevant nuclear war scenarios.

Fallout modeling and fatality estimates

The three silo fields near Yumen (40.1 N, 96.6 E), Hami (42.3 N, 92.5 E), and Ordos (40.1 N, 108.1 E) are respectively in the Gansu, Xinjiang, and Inner Mongolia regions of China (Figure 1). As of 15 January 2022, they comprised 120 silos at Yumen, 68 at Hami, and 82 at Ordos. While more silos could be added at each site in the future, we only consider these numbers for this first assessment.

For this study, we simulate the radiological impact of a simultaneous counterforce nuclear attack on the three silo fields. The attack consists of targeting each silo with 2 thermonuclear warheads of 300-kiloton of TNT yield each.[8] Nuclear explosions are assumed to take place at or near ground level (also known as ground bursts) and each generate a 14.2-km tall radioactive debris (or mushroom) cloud. The cloud is assumed to consist of micron-size silicate particles (density of 2.5 g/cm^3) exhibiting a log-normal size distribution with mean diameter of 0.407 micrometers and a geometric standard deviation of 4.[9] We then use a gravity-sorting algorithm to

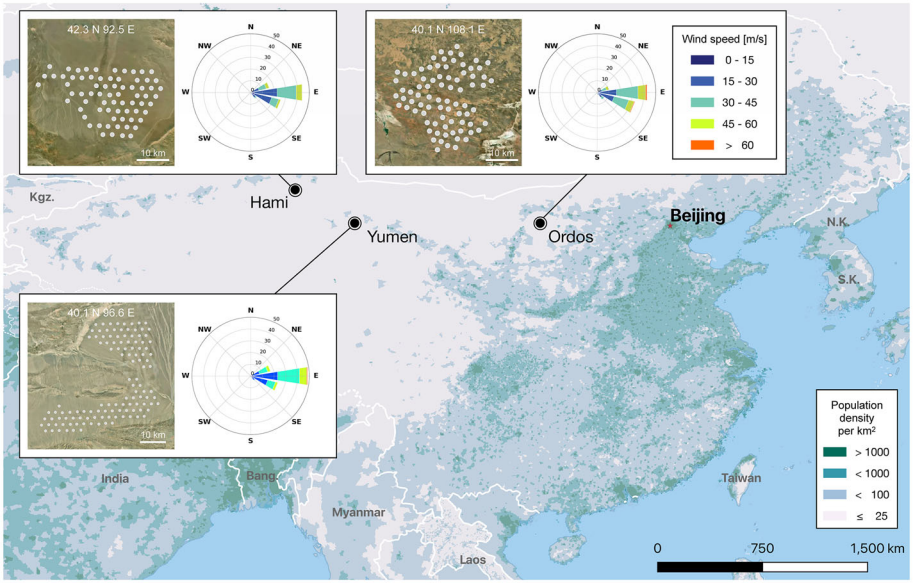

Figure 1. Locations and high-altitude wind speed and direction for the Yumen, Hami, and Ordos missile silo fields. Inserts provide the location of each silo under construction identified as of 15 January 2022 (Data from the Federation of American Scientists, background provided by Mapbox). The wind roses were produced with data from the Global Data Assimilation System one-degree weather archive and show the 2021 distribution of wind speed between 8 and 15 km altitude for 16 direction bins with probability percentiles of wind speed shown radially (and summing to 100). The directions are those into which the wind blows. The background map shows the local population density in person per km^2.

distribute the particles along the vertical axis of the stabilized cloud according to their size and the yield of the explosion.[10] Finally, the particles are distributed radially following a Gaussian distribution derived from the WSEG-10 fallout model.[11]

The resulting particle cloud is shown in Figure 2. About 80 percent of the initial activity is located within the cloud top (from 8 to 15-km altitude) at an altitude where winds are dominated by fast-flowing air currents (jet streams) blowing toward the east. Such winds are the most frequent (see annual and monthly data in Figures 1 and A1 respectively) and can carry radionuclides over hundreds of kilometers toward densely populated areas in less than two days.

To generate fallout deposition plumes, we use the NOAA HYSPLIT particle transport code together with weather data from the Global Data Assimilation System (GDAS1) one-degree archive to track the dispersion of the stabilized cloud particle distribution. The GDAS archive provides the necessary global atmospheric parameters to run HYSPLIT. The data is provided on a one-degree grid with a 3-hour daily temporal resolution.[12]

All the HYSPLIT input files (control and initial particle position files) for each detonation are generated by the Nuclear War Simulator (NWS)

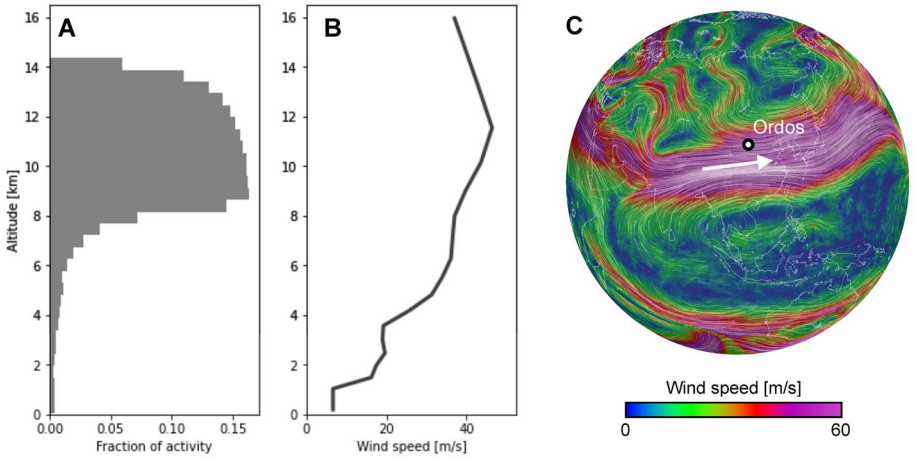

Figure 2. Initial activity distribution as a function of altitude and corresponding wind speed and direction for a stabilized cloud generated by a 300-kt ground-burst at Ordos on 15 December 2021. (A) About 80% of the initial activity present in the stabilized mushroom cloud is located between 8 and 15 km above ground level. (B) At such altitude, winds can reach speeds of 40–60 m/s. (C) Such winds result from fast flowing air currents (jet streams) blowing toward the east and can deliver the cloud particles hundreds of kilometers away within a few hours (here wind data at 300 hPa).

software. The simulations are then run locally using the standard HYSPLIT software distribution. To speed up calculations, the fallout from individual detonations can be run on multiple cores at the same time. HYSPLIT then tracks the ground deposition of radioactive particles over a given period (48h in our case) on a 0.00833 by 0.00833 degrees resolution grid. Because the total size of the grid has a large impact on the computation time and memory requirement for each run, NWS estimates and optimizes the dimensions of the required HYSPLIT grid span for the duration of the simulation using a simple fallout model based on the faster but less accurate WSEG-10 code.[13]

In HYSPLIT, particle deposition happens through gravitational settling and wet depletion consisting of within-cloud or below-cloud scavenging. The dry deposition velocity depends on the particle size, density, and form factor. Wet removal is defined as a scavenging coefficient expressed directly as a rate constant modified by the precipitation rate.[14] Once particle deposition is obtained, the results are post-processed in NWS to obtain iso-dose contour maps.

We integrate dose using time of arrival data in each grid cell, summed over all particle sizes, and use a traditional K-factor (or source normalization constant) approach to compute doses. Such an approach uses the exposure rate at H + 1 hour produced by the fallout from one kiloton of fission yield spread uniformly over a unit area. This dose rate is assumed

to decay according to a $t^{-1.2}$ power law.[15] The dose is obtained by integrating $t^{-1.2}$ from the particle deposition time to two weeks after detonation. Different K factors can be computed using different fission types, including fast and 14-MeV neutron induced fission in plutonium-239, uranium-235, and uranium-238. For our analysis, we used a K-factor of 6.1 10^7 (Gy/h)/(kT/m^2), corresponding to a fission products mixture generated from 14-MeV neutrons.[16] In addition, we assume that 50% of the total weapon yield results from fission.[17]

To compute fatalities, we compare the integrated dose with the local population density obtained from the European Union Commission Joint Research Center's Global Human Settlement Data set.[18] Both are computed on the same grid resolution (0.0083×0.0083) to improve computation speed. For a given individual, the probability of dying from acute radiation exposure is computed according to a probability distribution function such that individuals have a 50% chance of dying if exposed to 4.1 Gy of gamma radiation (see Figure A2).[19]

Because individuals may have the opportunity to shelter, the dose they receive is divided by a protection factor that accounts for the gamma attenuation provided by the type of dwelling (simple household, tall building, basement, fallout shelter…). Our model assumes different distributions of protection factors according to the local population density identifying rural ($d_{pop} < 100$ inhabitants per km^2), suburban ($100 < d_{pop} < 10000$ inhabitants per km^2), and urban ($d_{pop} > 10000$ inhabitants per km^2) areas (see data in Table A1). This accounts for the different types of shelter available to the population living in these different regions. We computed a distribution of protection factors for each population category by using the height of buildings as a proxy for each type of housing structures corresponding to standard protection factors available in the literature,[20] and by computing the distributions of building heights across mainland China as a function of population density. For the later, we relied on a recent building height dataset (1 km by 1 km resolution across China) produced by researchers from Peking University.[21]

Results and discussion

We simulated the radiological impact of 2-on-1 nuclear attacks (2 incoming warheads per silo) on the new Chinese missile silo fields and compute associated fatalities for each day of 2021. Our results were obtained by running about 1600 HYSPLIT simulations, with 300,000 3D particles each, representing together 8 weeks of CPU time.[22]

We find that inhabitants of major Chinese cities and provinces, including the capital Beijing (Figure 3) could receive two-week doses of radiation

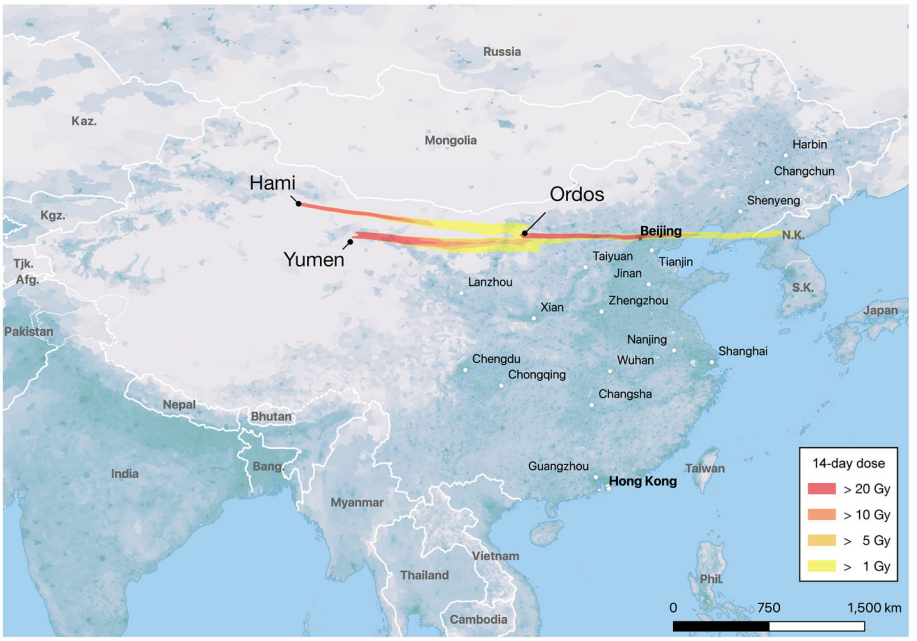

Figure 3. Outdoor fallout doses from 2-on-1 nuclear attacks on the Hami, Yumen and Ordos Missile silo fields. Two-week doses obtained with HYSPLIT for an attack on 15 December 2021 at 01:00 (UTC). Fallout patterns are overlaid on local population density. Fallout from attacks on the Ordos field could deliver lethal doses of radiation in the most densely populated areas including the capital Beijing. In this scenario, 25 million people could be at risk of receiving lethal doses of radiations and 9 million could die accounting for the protection provided by sheltering.

Table 1. Civilian fatalities estimates (in thousands) in China and neighboring countries from counterforce strikes on the new Chinese missile silo fields. Results are given for a 2 warheads on 1 silo attack scenario with and without protection factors.

	With protection factors			Without protection factors		
	Average	Standard deviation	Max	Average	Standard deviation	Max
China	4609.3	2102.8	13906.1	17922.1	8975.8	46643.0
North Korea	7.3	31.8	427.2	55.7	227.8	2907.9
South Korea	6.0	24.7	230.0	49.0	193.0	1730.6
Japan	1.6	12.1	178.2	14.7	104.0	1517.1
Mongolia	0.5	2.2	38.6	2.9	12.9	212.6

greater than 20 Gy resulting in millions of fatalities accounting for protection from sheltering.

Table 1 summarizes the average and maximum fatalities in China, North Korea, South Korea, Japan, and Mongolia. Average fatalities computed over one year would reach 4.6 ± 2.1 million deaths accounting for sheltering (18.0 ± 9.1 million without protection). We find that 70% of these fatalities would result from fallout from the Ordos field due to its relatively close and up-wind geographic location to densely populated areas.

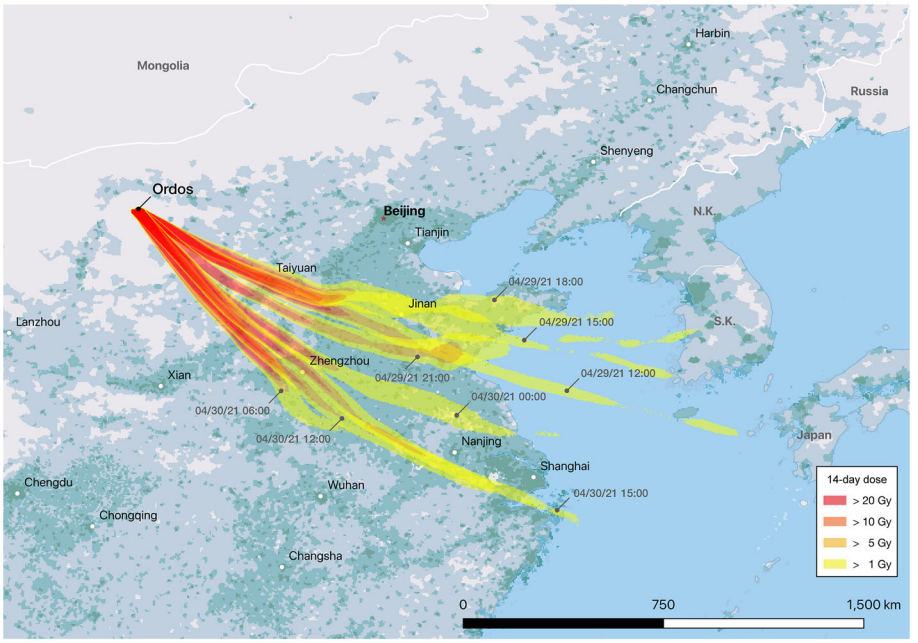

Figure 4. Outdoor fallout doses from 2-on-1 nuclear attacks on the Ordos field with winds blowing in the southeast direction. Each fallout plume was computed from 82 detonations on the Ordos field at different times of the day in the span of ~24 hours starting on 29 April 2021.

The spatial extents and directions of fallout are highly dependent on daily and hourly changes in wind patterns. Figure 4 shows that large areas south of the capital are equally at risk of fallout from attacks on the Ordos field (consistent with expected winds above Ordos, see Figure A1). Simulations with winds blowing toward the southeast (over the course of two days) suggests that inhabitants from cities with populations greater than 2 million such as Taiyuan, Zhengzhou, Jinan, Nanjing or even Shanghai could also receive lethal doses of radiation. Taiyuan and Zhengzhou, which are the closest to Ordos, could receive doses greater than 10 Gy. The others could receive doses in the 1 to 5 Gy range (with no protection), where mortality is rising sharply.

There are multiple sources of uncertainties associated with our fatality estimates. There are uncertainties about the particle source term and cloud height (as mentioned above, we use semi-empirical parameter values obtained from the literature). The fission yield of each detonation could vary from 0.3 (90 kiloton, 50% fission fraction) to 2.4 (455 kiloton with 80% fission) times the value we picked (300 kiloton, 50% fission). We currently omit radiation doses from activation products as well as any doses resulting from immersion in the radioactive cloud, inhalation of radioactive particles, and ingestion of potentially contaminated water and food.

Additional silos and command and control centers under construction could also be targeted and increase the amount of fallout.

Perhaps most importantly, we assumed that the nuclear explosions aimed at destroying the silos, which are hard targets, would be ground bursts. This type of explosion generates the most amount of fallout. There are new types of fuses, however, that improve the lethality of warheads by making the destruction of silos possible by detonating within a certain volume above the target.[23] While above ground detonations up to 300 m altitude would generate less local fallout, their radiological impact would still be significant because the fireballs from the nuclear explosions would still interact partially with the ground. The fallout effect of this partial interaction can be estimated by assuming that low altitude bursts generate only a fraction f_d of the fallout from ground bursts, with f_d being a function of both the yield and altitude of detonation.[24] We find that for a hard silo target (10,000 psi or ~70 MPa blast pressure), f_d ranges from ~0.25 to 1, with an average value of 0.5 for a 10,000 psi "kill" volume independent of yield.[25]

There is no guarantee that the incoming warheads would detonate above ground, however. In a 2 warheads on 1 silo attack scenario, military planners may still wish to detonate the second warhead at ground level because of the likelihood that the first low altitude burst may modify the local topography of the target in an unpredictable manner. Ultimately, whether advanced fuses are used or not, and incoming warhead explode on or near the surface, the resulting fallout could still lead to the death of millions of civilians.

Conclusion

China's recent nuclear weapon build-up is likely to affect U.S. nuclear posture and war plans and contribute to limiting the scope of further nuclear arms reduction between the United States and Russia. As we have shown in this study, it puts Chinese citizens at greater risk of being exposed to lethal dose of radiation in scenarios where the intended targets are nuclear weapon systems.

Our simulations of fallout from counterforce strikes on the new missile silo fields show that more than 14 million people could die in China as unintended but expected humanitarian consequences. They also highlight transboundary radiological risks from counterforce strikes as North Korea, South Koreas, Japan, and Mongolia could all face significant fatalities. In our scenarios, fatalities would largely be dominated by fallout from the Ordos field, as its geographic location and local high-altitude wind patterns blowing toward the east or southeast favor the transport of radioactive

particles toward the most densely populated areas and cities of China, including its capital Beijing.

We note that we only calculate mortality numbers from acute radiation sickness. Many more would suffer from long-term effects of radiation exposure and die prematurely. Additional attacks on already existing deployed Chinese nuclear weapon systems would certainly raise this figure further. Our findings confirm the grave risks associated with siting and attacking large silo fields upwind from densely populated areas and should prompt policymakers to re-evaluate the prudence of such decisions.

Notes

1. Warrick, Joby, "China is Building more than 100 New Missile Silos in its Western Desert, Analysts Say," *Washington Post*, 30 June 2021; Korda, Matt and Hans Kristensen, "China is Building a Second Nuclear Missile Silo Field," *The Strategic Security Blog,* Federation of American Scientists, 26 July 2021, https://fas.org/blogs/security/2021/07/china-is-building-a-second-nuclear-missile-silo-field/; Broad, William J. and David E. Sanger, "A 2nd New Nuclear Missile Base for China, and Many Questions about Strategy," *New York Times* (26 July 2021); Lee, Rod, "PLA Likely Begins Construction of an Intercontinental Ballistic Missile Silo Site near Hanggin Banner," *China Aerospace Studies Institute*, 12 August 2021, https://www.airuniversity.af.edu/CASI/Display/Article/2729781/pla-likely-begins-construction-of-an-intercontinental-ballistic-missile-silo-si/. In addition to the three identified silo sites, China has also built an important ICBM training site at Jilantai, which may achieve some operational capabilities. See: Hans Kristensen, "China's Expanding Missile Training Area: More Silos, Tunnels, and Support Facilities," *The Strategic Security Blog,* Federation of American Scientists, 24 February 2021, https://fas.org/blogs/security/2021/02/plarf-jilantai-expansion/.
2. Silo coordinates were obtained from the Federation of American Scientists, Data as of 15 January 2022. See: https://public.tableau.com/app/profile/kate.kohn/viz/YumenMissileSiloField/Dashboard1; https://public.tableau.com/app/profile/kate.kohn/viz/HamiMissileSiloField/Dashboard1; https://public.tableau.com/app/profile/kate.kohn/viz/OrdosMissileSiloField/Dashboard1.
3. U.S. Central Command recently disclosed the presence of a U.S. ballistic missile submarine (SSBN) in the Arabian sea. From such a station, a U.S. SSBN could target China's new missile silo fields without flying missiles above Russia. See: Moriyasu, Ken. "Stealthiest U.S. submarine makes rare appearance in Arabian Sea," *Nikkei Asia*, 20 October 2022.
4. Drell, Sidney D., and Frank Von Hippel. "Limited Nuclear War," *Scientific American* 235, no. 5 (1976): 27–37; Von Hippel, Frank N., Barbara G. Levi, Theodore A. Postol, and William H. Daugherty, "Civilian Casualties from Counterforce Attacks," *Scientific American* 259 (1988): 36–43; McKinzie, Matthew, Thomas B. Cochran, Robert S. Norris, and William M. Arkin, *The U.S. Nuclear War Plan: A Time for Change* (Washington, DC: Natural Resources Defense Council, 2001), 1–198; Helfand, Ira, Lachlan Forrow, Michael McCally, and Robert K. Musil, "Projected US Casualties and Destruction of US Medical Services from Attacks by Russian Nuclear Forces," *Medicine & Global Survival* 7 (2002): 68–76.

5. Rolph, G. D., F. Ngan, and R. R. Draxler, "Modeling the Fallout from Stabilized Nuclear Clouds using the HYSPLIT Atmospheric Dispersion Model," *Journal of environmental radioactivity* 136 (2014): 41–55; Philippe, Sébastien, Sonya Schoenberger, and Nabil Ahmed, "Radiation Exposures and Compensation of Victims of French Atmospheric Nuclear Tests in Polynesia," *Science and Global Security* 30 (2022): 1–33, DOI: 10.1080/08929882.2022.2111757.
6. Stein, A.F., Draxler, R.R, Rolph, G.D., Stunder, B.J.B., Cohen, M.D., and Ngan, F., "NOAA's HYSPLIT Atmospheric Transport And Dispersion Modeling System," *Bulletin of the American Meteorological Society* 96 (2015): 2059–2077, http://dx.doi.org/10.1175/BAMS-D-14-00110.1
7. Ivan Stepanov, Nuclear War Simulator, build 394, www.nuclearwarsimulator.com
8. This yield is typical of the U.S. arsenal. The silo-based LMG-30G Minuteman III intercontinental ballistic missiles carry 300-kiloton warheads and Sea-launched ballistic missile carry warheads in the 90 to 455-kiloton range, see: Kristensen, Hans M., and Matt Korda, "United States Nuclear Weapons, 2021," *Bulletin of the Atomic Scientists* 77 (2021): 43–63.
9. The size, surface and volume of fallout particles are all log-normally distributed. Each representing the 1st, 2nd, and 3rd moments of the distribution, respectively. We use the 2.5 moment of the distribution to model to a first order the effect of fractionation between refractive and volatile nuclide who are typically located within the particle volume and on the particle surface, respectively. See Bigelow Jr, Winfield S. Far field fallout prediction techniques. Air Force Institute of Technology, PhD Thesis, 1983, 1–172, https://apps.dtic.mil/sti/pdfs/ADA151871.pdf. For our particle source term, we use the DELFIC mean diameter and standard deviation for ground bursts (obtained from particle measured at the U.S. Nevada test site) dividing the size-distribution into 100 size bins such that the integrated activity within each bin is equal. The inverse cumulative distribution function is used to determine the minimum and maximum particle size of each bin. The representative particle size of each bin is then calculated as the geometrical mean of the edges of the bin. See Norment, Hillyer G., "DELFIC: Department of Defense Fallout Prediction System. Volume I-Fundamentals," Atmospheric Science Associates, Bedford MA, 1979, 1–101, available at https://apps.dtic.mil/sti/pdfs/ADA088367.pdf.
10. The spatial distribution of cloud particle is obtained from the model developed by Conners, Stephen P., "Aircrew Dose and Engine Dust Ingestion from Nuclear Cloud Penetration," Air Force Institute of Technology, PhD Thesis, 1985, 82–83, https://apps.dtic.mil/sti/pdfs/ADA159246.pdf
11. For a yield of 300 kT, the standard deviation is about 2 km. See Hanifen, Dan W. Documentation and Analysis of the WSEG-10 Fallout Prediction Model. Air Force Institute of Technology, 1980, 7 and Edward Geist, GLASSTONE-nuclear weapons effects modelling in Python, 15 August 2019, https://github.com/GOFAI/glasstone
12. The GDAS data is also available on a 0.5 by 0.5 and 0.25 by 0.25 degree-grids. We use the 1-degree grid to optimize storage space as we run HYSPLIT locally. See, NOAA Air Resources Laboratory (ARL), "Global Data Assimilation System (GDAS1) Archive Information," (2004). https://www.ncei.noaa.gov/products/weather-climate-models/global-data-assimilation
13. See Hanifen, Dan W., "Documentation and Analysis of the WSEG-10 Fallout Prediction Model," Air Force Institute of Technology, 1980, 1–105 and Edward Geist, GLASSTONE-nuclear weapons effects modelling in Python, 15 August 2019, https://github.com/GOFAI/glasstone

14. In HYSPLIT, wet removal is defined as $\beta_{wet} = 8 \times 10^{-5}\ P^{0.79}$ with P the precipitation rate in mm/h. We used the HYSPLIT default scavenging coefficient (8×10^{-5}), applied both to below and within-cloud scavenging, which apply to a wide range of particle sizes. See Sportisse, Bruno, "A Review of Parameterizations for Modelling Dry Deposition and Scavenging of Radionuclides," *Atmospheric Environment* 41 (2007): 2683–2698.
15. This method has been used for example in earlier iteration of the U.S. DOE DELFIC fallout prediction code. See: Norment, Hillyer G., "DELFIC: Department of Defense Fallout Prediction System," Volume I-Fundamentals, op.cit.
16. Standard values for K are available from the 1979 DELFIC source code. Typical values range from 6.11 10^7 to 7.2 10^7 (Gy/h)/(kT/m^2) depending on the nuclide and the fission energy. See: Norment, Hillyer G. DELFIC: Department of Defense Fallout Prediction System. Volume II. User's Manual. Atmospheric Science Associates, Bedford MA, 1979, 161, and Bigelow Jr, Winfield S., "Far Field Fallout Prediction Techniques," III-4.
17. This is sometimes referred as a 50% fission fraction in the literature. See, McKinzie, Matthew et al., "The U.S. Nuclear War Plan: A Time For Change," Op. cit.
18. Florczyk, Aneta J., Christina Corbane, Daniele Ehrlich, Sergio Freire, Thomas Kemper, Luca Maffenini, Michele Melchiorri et al., "GHSL Data Package 2019," Luxembourg, EUR 29788, no. 10.2760 (2019): 290498.978-92-76-13186-1, doi:10.2760/290498, JRC 117104
19. McClellan, Gene, David Crary, and Darren Oldson, *Approximating the Probability of Mortality Due to Protracted Radiation Exposures*. DTRA-TR-16-054, Applied Research Associates, Inc. Arlington United States, 2016.
20. Buddemeier, B. R., and M. B. Dillon, "Key Response Planning Factors for the Aftermath of Nuclear Terrorism," No. LLNL-TR-410067. Lawrence Livermore National Lab (LLNL), Livermore, CA (United States), 2009.
21. Yang, Chen, and Shuqing Zhao, "A Building Height Dataset Across China in 2017 Estimated by the Spatially-Informed Approach," *Scientific Data* 9 (2022): 1–11.
22. We ran 365 counterforce attacks twice for each day of the year (once with all silo fields and once with Ordos only) as well as 10 attacks on each silo of the Ordos field in the span of 24H on 29 April 2021 (820 simulations in total).
23. Kristensen, Hans M., Matthew McKinzie, and Theodore A. Postol, "How US Nuclear Force Modernization is Undermining Strategic Stability: The Burst-Height Compensating Super-Fuze," *Bulletin of the Atomic Scientists*, March 1, 2017, https://thebulletin.org/2017/03/how-us-nuclear-force-modernization-is-undermining-strategic-stability-the-burst-height-compensating-super-fuze/
24. We use a semi-empirical model based on data from U.S. atmospherics test fallout in Nevada with $f_d = 0.45345^{\lambda\backslash 65}$ where $\lambda = (h/Y^{1/3})$ is the scaled height of burst in feet per $kT^{1/3}$. See, Norment, "DELFIC: Department of Defense Fallout Prediction System," Volume I-Fundamentals, 53.
25. For the dimensions of the 10,000 psi kill volume, see Glasstone, Samuel and Philip J. Dolan, *The effects of nuclear weapons,* U.S. Department of Defense, 1977, 111.
26. We extracted data from the GDAS1 weather archive using the ARLreader python package, see Martin Radenz, Yin Zhenping, ARL reader, 29 April 2020, https://github.com/martin-rdz/ARLreader
27. McClellan, Gene, David Crary, and Darren Oldson. *Approximating the Probability of Mortality Due to Protracted Radiation Exposures*. DTRA-TR-16-054, Applied Research Associates, Inc. Arlington United States, 2016.

Acknowledgements

The authors gratefully acknowledge the NOAA Air Resources Laboratory (ARL) for the provision of the HYSPLIT transport and dispersion model used in this publication. Figures 1, 3, and 4 use map data from Mapbox and OpenStreetMap and their data sources. Figure 2 use data from C. Beccario (https://earth.nullschool.net/). We thank Frank von Hippel and Zia Mian for useful discussions and feedback on the manuscript.

Disclosure statement

Ivan Stepanov is the lead developer of the Nuclear War Simulator, a commercial software published by Slithering Software UK Ltd used in this study. Sébastien Philippe declares no conflicts of interest.

Code availability statement

The source code for the HYSPLIT transport and dispersion model is available upon request from the NOAA Air Resources Laboratory (https://www.ready.noaa.gov/HYSPLIT_linux.php).

ORCID

Sébastien Philippe http://orcid.org/0000-0002-7282-7520

Data availability statement

All data generated or analyzed during this study are either included or cited in the published article and are available from the corresponding author upon reasonable request.

Appendix A. Additional data and figures

Table A1. Protection factors for rural, suburban, and urban populations.

	Class 1	Class 2	Class 3	Class 4	Class 5	Class 6	Class 7	Class 8	Average
Rural	1.0	2.5	3.0	3.0	3.0	3.0	3.0	7.2	3.2
Suburban	1.0	2.9	3.0	3.0	3.0	5.7	7.0	10.6	4.5
Urban	1.0	4.2	7.0	7.7	10.0	10.0	13.0	19.1	9.0

Each population is divided in 8 classes, representing 12.5% of the population in each category. Protection factors were computed based on population and building height densities in rural, suburban, urban areas across China.

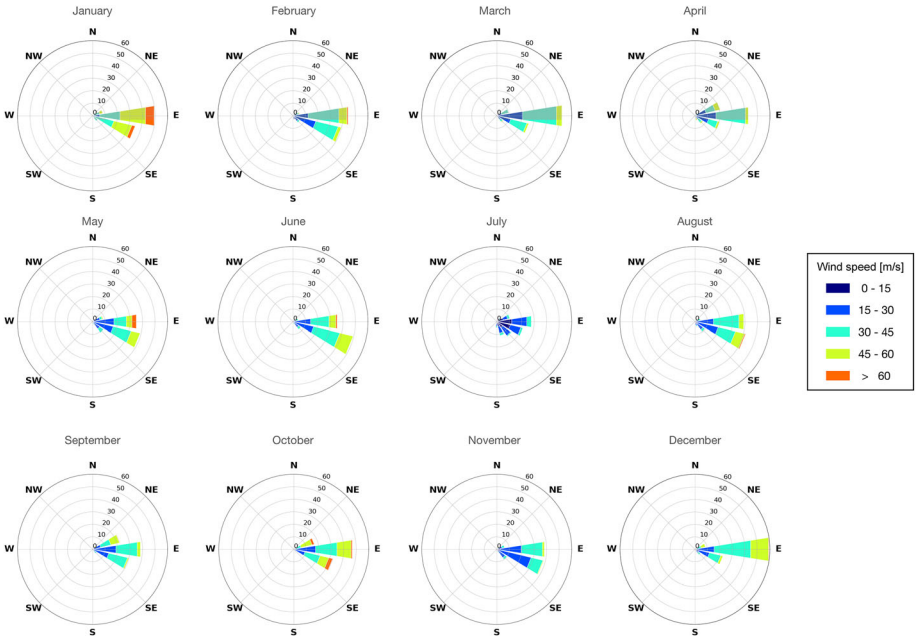

Figure A1. Monthly wind patterns between 8 and 15 km above the Ordos field for the year 2021. Monthly average wind direction and speed between 100 and 300 hPa were computed for Ordos (40.062 N, 108.107 E) using the GDAS1 dataset.[26] The directions are those into which the wind blows.

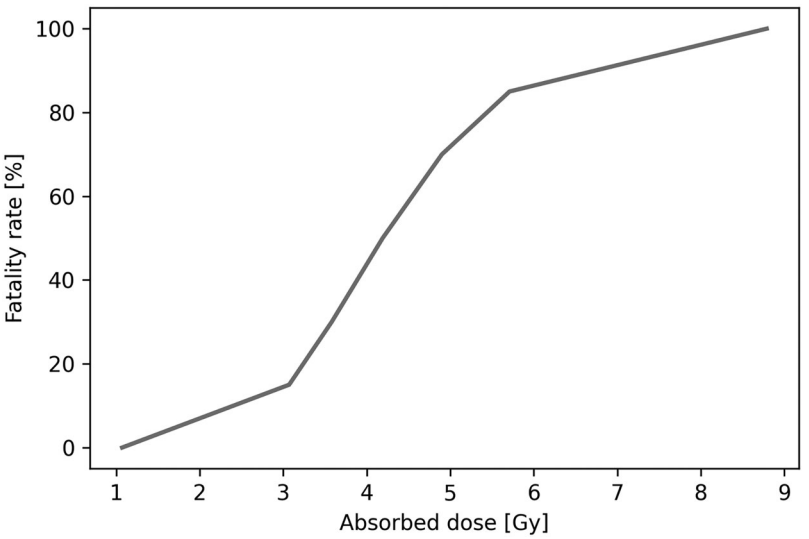

Figure A2. Fatality rate from acute radiation syndrome as a function of the integrated radiation dose received.[27]